Research on infrared fault warning method of hotline tap clamp of substation equipment based on hybrid segmentation

Shen Peifeng[1], Yang Yang[*2], Li Yong[1], Li Lihua[2], Chen Ting[1], and Yang Ning[1]

[1]Taizhou Power Supply Branch of Jiangsu Electric Power Company, No.2 Fenghuang West Road, Taizhou, China
E-mail: 15052826688@163.com
[2]China Electric Power Research Institute, No.15 Xiaoyingdonglu, Beijing, China
E-mail: yang.yang_epri@qq.com

Abstract. The occurrence of substation equipment faults is usually associated with the heating of equipment components. Hotline tap clamps of substation equipment are important parts for carrying load currents and key parts for thermal fault potential. Therefore, a new hybrid early warning method for infrared faults of hotline tap clamp of substation equipment is proposed. A two-dimensional Otsu algorithm is used for coarse segmentation of infrared images to reduce the complexity of subsequent fine segmentation. Since the CV (Chan-Vese model) model is not accurate enough for image segmentation with uneven grayscale. The differential information obtained by the Prewitt operator to detect the target edges is combined with CV model to improve the segmentation accuracy, and the fine segmentation of hotline tap clamp of substation equipment is achieved by the improved CV model. The temperature information is applied to the segmented images, and the fault warning of the hotline tap clamp of substation equipment is realized based on the relative temperature difference. The experimental results show that the method can improve the segmentation effect of infrared images and achieve the purpose of fault warning.

Keywords: Infrared images, Image segmentation, Two-dimensional Otsu, CV model, Prewitt operator, Fault warning

1. INTRODUCTION

Nowadays, the demand for electric energy in national production and life is gradually increasing, and the scale of the power grid is also increasing. The power equipment in substations is an important part of maintaining the safe operation of the power grid, and its safety and reliability directly affect the safety and stability of the power system. According to statistical data [1, 2], many faults in the power system are directly related to power equipment failures, and the abnormal temperature phenomenon of the equipment will appear at the early stage of power equipment failure [3, 4]. The hotline tap clamp of substation equipment is important part for carrying load currents and are also key part for potential thermal fault. To improve the safety and reliability of the power grid, infrared diagnostic technology is used for fault warning of hotline tap clamp for the substation. However, complex environment and background interference make it hard to obtain the target area for fault diagnosis of substation equipment [5, 6]. Therefore, it is important to effectively segment hotline tap clamp from infrared thermal image to achieve infrared monitoring of power equipment temperature and prevent equipment faults at the early stage. At present, numerous scholars have conducted various researches on fault diagnosis of substation equipment by infrared imaging technology. Ying proposed the segmentation of infrared images of substation equipment using the traditional Otsu method, and detected images with abnormal hot spots[7]. Gu proposed a level set segmentation method based on an improved CV model. He added local terms to handle local region information as well as symbolic distance energy penalty terms to segment out the infrared images accurately[8]. Wang improved the region growing method using two-dimensional Otsu threshold segmentation method. He extract the complete target device from the complex background images and diagnose the device region structure based on the extreme value law of the pixel statistical map of the extracted device and the fault diagnosis criterion[9]. Chen used gamma change and Retinex algorithm to enhance the infrared images of substation equipment and segmented more complete power equipment using multi-scale structural smoothing filters[10]. These studies have made certain contributions but still cannot achieve good segmentation accuracy for substation equipment infrared images with complex backgrounds and severe noise. There is still a large room for improvement in the combination of the algorithm's resistance to thermal noise and the need for thermal fault warning. Therefore, this paper proposes a new method to achieve early warning of faults for infrared images of substation equipment with complex backgrounds. A two-dimensional Otsu algorithm is used to achieve coarse segmentation of the background and foreground targets. Since the Prewitt operator can calculate the gray value and detect the edge information of the target using the differential information of the image [11], the Prewitt operator is combined into CV model. The features obtained from the coarse segmentation are used as the initial conditions to improve CV model to achieve the fine segmentation of the hotline tap clamp of substation

equipment. The temperature information is introduced to the segmented area, and the hotline tap clamp of substation equipment is judged based on the relative temperature difference method [12] to achieve early warning of substation equipment faults.

2. PRINCIPLE OF THE SPLITTING ALGORITHM

2.1. Two-dimensional Otsu algorithm

Otsu algorithm has the advantages of being computationally simple, stable and highly adaptive in image segmentation [13]. However, the Otsu algorithm does not make use of the local spatial information of the image, which can lead to unsatisfactory image segmentation when there is noise interference and grey-scale cross distribution in the images [14].Therefore, Liu [15] proposed a two-dimensional Otsu algorithm with full consideration of the pixel points themselves as well as the neighborhood grey scale values, which improves the noise suppression performance of the algorithm with good anti-interference and high self-adaptability.

Two-dimensional Otsu algorithm for an image with a grey level of L and dimensions $M \times N$. A two-dimensional attribute histogram[16] is constructed using the mean neighborhood grey level $g(x,y)$ and the pixel point grey level $f(x,y)$. And a binary optimal threshold (S,T) is calculated for the target and background with the maximum dispersion between classes as the objective function.

The mean grayscale value $g(x,y)$ in a $k \times k$ neighborhood centered at $(x,y)$is calculated as:

$$g(x,y)=\frac{1}{k\times k}\sum_{m-(k-1)/2}^{(k-1)/2}\sum_{n-(k-1)/2}^{(k-1)/2} f(x+m,y+n) \quad (1)$$

where $0<x+m<M$, $0<\mathrm{y}+n<N$. k generally takes odd numbers.

Suppose the two-dimensional attribute histogram as shown in **Fig.1**, where regions A and C are the target and background respectively. Regions B and D are the edge points and noise respectively.

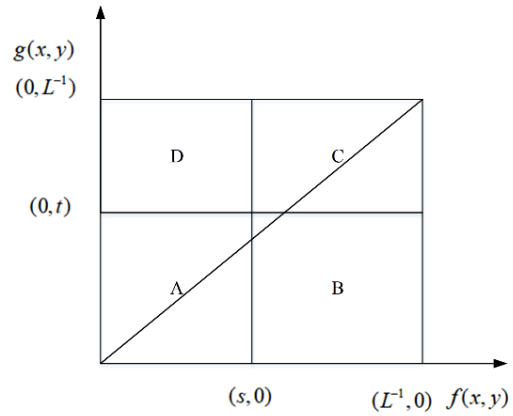

Fig.1 Average grayscale two-dimensional histogram

Suppose c_{ij} denotes the frequency of occurrences of a pixel point with a grey value i , and a mean grey value in its neighborhood is j . Its two-dimensional joint probability density p_{ij} is obtained as:

$$p_{ij}=\frac{c_{ij}}{M\times N} \quad (2)$$

where $0\le i\le L-1$, $0\le j\le L-1$.

The probability of its target region is $w_0=\sum_{i=0}^{s}\sum_{j=0}^{t}p_{ij}$ and the probability of its target background is $w_1=\sum_{i=s+1}^{L-1}\sum_{j=0}^{t}p_{ij}$.

The corresponding mean vectors μ_0 and μ_1 of the target and background for the 2D attribute histogram at this point are:

$$\mu_0=\begin{bmatrix}\mu_{0i} & \mu_{0j}\end{bmatrix}^T=\begin{bmatrix}\sum_{i=0}^{s}\sum_{j=0}^{t}\frac{ip_{ij}}{w_0} & \sum_{i=0}^{s}\sum_{j=0}^{t}\frac{jp_{ij}}{w_0}\end{bmatrix}^T \quad (3)$$

$$\mu_1=\begin{bmatrix}\mu_{1i} & \mu_{1j}\end{bmatrix}^T=\begin{bmatrix}\sum_{i=s+1}^{L-1}\sum_{j=0}^{t}\frac{ip_{ij}}{w_1} & \sum_{i=s+1}^{L-1}\sum_{j=0}^{t}\frac{jp_{ij}}{w_1}\end{bmatrix}^T \quad (4)$$

where μ_{0i} and μ_{0j} are the grey scale value of the target class and the neighborhood average grey scale value, respectively; μ_{1i} and μ_{1j} are the grey scale value of the background class and the neighborhood average grey scale value, respectively.

The total mean vector of the two-dimensional attribute histogram at this point is:

$$u_T=\begin{bmatrix}\mu_{ti} & \mu_{tj}\end{bmatrix}^T=\begin{bmatrix}\sum_{i=0}^{L-1}\sum_{j=0}^{t}ip_{ij} & \sum_{i=0}^{L-1}\sum_{j=0}^{t}jp_{ij}\end{bmatrix}^T \quad (5)$$

where μ_{ti} and μ_{tj} are the overall grey value and the neighborhood average grey value, respectively. The inter-class dispersion matrix S_B for the target and background is:

$$S_B=w_0(\mu_0-\mu_T)(\mu_0-\mu_T)^T+w_1(\mu_1-\mu_T)(\mu_1-\mu_T)^T \quad (6)$$

Trace $tr[S_B(s,t)]$ of the interclass dispersion matrix as a measure of dispersion:

$$\begin{aligned}tr[S_B(s,t)]=w_0\left[\left(\mu_{0i}-\mu_{Ti}\right)^2+\left(\mu_{0i}-\mu_{Tj}\right)^2\right]\\+w_1\left[\left(\mu_{1i}-\mu_{Ti}\right)^2+\left(\mu_{1j}-\mu_{T_j}\right)^2\right]\end{aligned} \quad (7)$$

The binary optimal threshold (S,T) is obtained when the trace of the inter-class dispersion matrix is maximum as in equation (8):

$$(S,T)=\arg\max_{1\le s,t\le L}\left\{tr\left[S_{\mathrm{B}}(s,t)\right]\right\} \quad (8)$$

2.2. CV model

CV model is a region-based level set method based on the Mumford-Shah model [17], which is a simplification of the Mumford-Shah model to improve the computational accuracy by raising the computation from N to N+1 dimensions [18-21]. If the image $u_0(\mathrm{x},\mathrm{y})$in a given image domain Ω is divided into two regions,

target C and background C, by a closed curve C, the main form of the energy generalization of CV model is as follows:

$$\begin{aligned} E(C) &= E_1(C) + E_2(C) \\ &= \iint_{\text{inside}(C)} |u_0(x,y) - c_1|^2 \, \mathrm{d}x\mathrm{d}y \\ &+ \iint_{\text{outside}(C)} |u_0(x,y) - c_2|^2 \, \mathrm{d}x\mathrm{d}y \end{aligned} \tag{9}$$

where c_1 is the mean of the grey levels in the inner region of curve C and c_2 is the mean of the grey levels in the outer region of curve C. The first and second terms in the energy generalization are fitting terms that allow the closed curve C to evolve towards the target profile.

Usually, the constrained energy terms of length and area are added to the energy generalization corresponding to CV model, to ensure that the resulting energy profile is short and smooth enough, as follows:

$$\begin{aligned} E(C, c_1, c_2) &= \mu \cdot L(C) + \eta \cdot S(C) \\ &+ \lambda_1 \iint_{\text{inside}(C)} |u_0(x,y) - c_1|^2 \, \mathrm{d}x\mathrm{d}y \\ &+ \lambda_2 \iint_{\text{outside(C)}} |u_0(x,y) - c_2|^2 \, \mathrm{d}x\mathrm{d}y \end{aligned} \tag{10}$$

where, $\mu \geq 0$, $\eta \geq 0$, $\lambda_1, \lambda_2 > 0$ are fixed parameters, and in numerical calculations, it is common to define $\lambda_1 = \lambda_2 = 1$ and $\eta = 0$. The evolution of the closed curve C towards the target edge is driven by calculating the squared error between the grey value of the target area image and c_1, and the squared error between the grey value of the background area image and c_2.

Let function $\phi(x,y)$ be the initial zero level set curve constructed on the basis of the closed curve C. Define regularized Heaviside function $H(\phi)$ and Dirac function $\delta(\phi)$ as follows:

$$\begin{cases} H_\varepsilon(z) = \dfrac{1}{2}\left(1 + \dfrac{2}{\pi}\arctan\left(\dfrac{z}{\varepsilon}\right)\right) \\ \delta_\varepsilon(z) = \dfrac{1}{\pi}\dfrac{\varepsilon}{\varepsilon^2 + z^2}, z \in R \end{cases} \tag{11}$$

From this, the expression for the level set corresponding to equation (12) is obtained as:

$$\begin{aligned} E(c_1, c_2, \varphi) &= \mu \iint \delta_\varepsilon(\varphi(x,y)) \, |\nabla\varphi(x,y)| \, dxdy \\ &+ \lambda_1 \iint_\Omega |u_0(x,y) - c_1|^2 \, H_\varepsilon(\varphi(x,y)) dxdy \\ &+ \lambda_2 \iint_\Omega |u_0(x,y) - c_2|^2 \times (1 - H_\varepsilon(\varphi(x,y))) dxdy \end{aligned} \tag{12}$$

This level set expression is minimized and its corresponding Euler-Lagrange equation is solved to obtain the steepest gradient descent flow as:

$$\frac{\partial\varphi}{\partial t} = \delta_\varepsilon(\varphi)\left[\mu \bullet div\left(\frac{\nabla\varphi}{|\nabla\varphi|}\right) - \lambda_1(u_0 - c_1)^2 + \lambda_2(u_0 - c_2)^2\right] \tag{13}$$

where ∂t is the time step, and $div\left(\dfrac{\nabla\varphi}{|\nabla\varphi|}\right)$ is the curvature of the level set surface. And each evolution requires an update of c_1 and c_2, where c_1 and c_2 are constants defined as follows:

$$\begin{cases} c_1(\phi) = \dfrac{\iint_\Omega u_0(x,y) H_\varepsilon(\varphi(x,y)) dxdy}{\iint_\Omega H_\varepsilon(\varphi(x,y)) dxdy} \\ c_2(\phi) = \dfrac{\iint_\Omega u_0(x,y)(1 - H_\varepsilon(\varphi(x,y))) dxdy}{\iint_\Omega (1 - H_\varepsilon(\varphi(x,y))) dxdy} \end{cases} \tag{14}$$

The level set is approximately a partial differential equation that iteratively updates the target detection profile using the time parameter as a variable, and the target area profile is obtained after the extraction of the zero-level set is completed.

3. Algorithm of This Paper

In this paper, infrared images taken by FLIR thermal imager are used as input. Firstly, the IR image is pre-processed with median filtering and grayscale, and then the temperature matrix is obtained by FLIR Tools. The pre-processed image is separated from the background by a two-dimensional Otsu algorithm basically. The features obtained from coarse segmentation are used as the initial conditions of the improved CV model to achieve fine segmentation of hotline tap clamp of substation equipment. The temperature information is mapped to the segmented area, and the early warning of substation equipment fault is realized according to the relative temperature difference judgment method. The algorithm flow is shown in **Fig.2**:

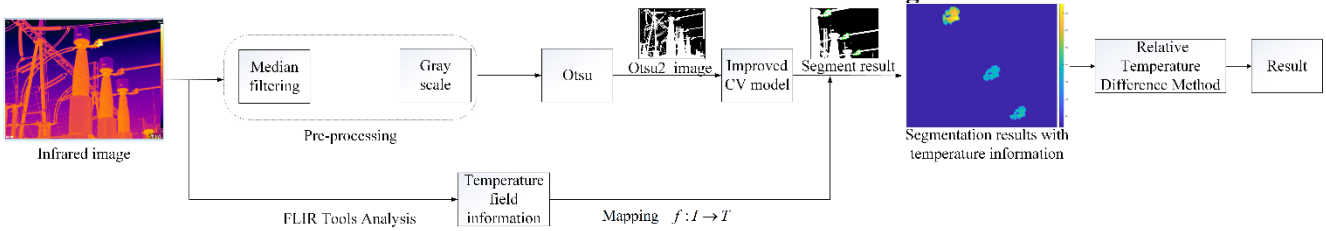

Fig.2 Algorithm Flow Diagram

3.1. CV model Combined with Prewitt Operator

-1	-1	-1
0	0	0
1	1	1

(a)x direction

-1	0	1
-1	0	0
-1	0	1

(b)y direction

Fig.3 Filter template of Prewitt operator

In CV model, the level set was firstly initialized. Then the average gray of foreground and background were calculated respectively based on the initialized level set, and the average gray of foreground and background were used to evolve each pixel of the level set finally. The average gray of the inside and outside contour was used as the level set expression in CV model, so it is easy to segment images with the uniform global gray distribution. However, in infrared images, the edges have an uneven distribution of gray values, and the segmentation of the target using CV model is not effective in this case. Therefore, in the process of segmenting infrared images using CV model, the gray value of each pixel point in the image with differential information is calculated using the Prewitt operator. The difference is calculated as the gray value of each pixel point in the image. It can extract the edge information of the image and effectively segment the image with an uneven grayscale. The Prewitt operator performs the differencing operation on the x-direction and y-direction of the image pixel points respectively. Fig. 3 shows the filtering template of the Prewitt operator in x and y-direction and convolves the image with odd-sized kernels in the vertical and horizontal directions respectively. When the kernel size is 3, the result of the operation for each pixel is as follows:

$$G_x = \begin{pmatrix} -1 & -1 & -1 \\ 0 & 0 & 0 \\ +1 & +1 & +1 \end{pmatrix} * I \tag{15}$$

$$G_y = \begin{pmatrix} -1 & 0 & +1 \\ -1 & 0 & +1 \\ -1 & 0 & +1 \end{pmatrix} * I \tag{16}$$

where G_x and G_y denote the grayscale values obtained from edge detection in horizontal and vertical directions respectively, and then the approximate gradient can be obtained by combining G_x and G_y:

$$G = \sqrt{G_x^2 + G_y^2} \tag{17}$$

where G is the gray value of the differential information at each pixel, and the energy function of the improved CV model is as follows:

$$\begin{aligned} E(C, c_1, c_2) &= \mu \cdot L(C) + \eta \cdot S(C) \\ &+ \lambda_1 \iint_{\text{inside}(C)} |u_0(x,y) - s_1|^2 \, \mathrm{d}x\mathrm{d}y \\ &+ \lambda_2 \iint_{\text{outside}(C)} |u_0(x,y) - s_2|^2 \, \mathrm{d}x\mathrm{d}y \end{aligned} \tag{18}$$

where s_1 and s_2 are the mean grayscale values with differential information inside and outside the contour, and they are operated by the Prewitt operator. The energy function is minimized by solving the corresponding Euler-Lagrange equation.

3.2. Fault waring

The temperature matrix is obtained by the analysis of the infrared image of the input substation equipment by FLIR Tools, and the segmentation results obtained from the improved segmentation model are mapped to the temperature matrix according to the equation $f: I \to T$ to obtain the temperature information of the segmentation results. After that, the segmented area with temperature information is diagnosed by using the relative temperature difference judgment method. The relative temperature difference is defined as follows: the percentage of the difference between the temperature rise of two corresponding measurement points and the ratio of the temperature rise of the higher temperature point. The relative temperature difference δ can be found by the following equation.

$$\delta = (\tau_1 - \tau_2)/\tau_1 \times 100\% = (T_1 - T_2)/(T_1 - T_0) \times 100\% \tag{19}$$

where τ_1 and T_1 are the temperature rise and temperature of the hot spot, respectively; τ_2 and T_2 are the temperature rise and temperature at normal correspondence points, respectively; T_0 is the temperature of the reference environment.

When using the relative temperature difference judgment method to measure the relative temperature difference $\delta \geq 35\%$ in the hotline tap clamp of substation equipment, the equipment is a failure, then the relevant technical personnel should be arranged as soon as possible to overhaul the equipment.

4. Experimental Results and Analysis

The experiments were carried out in the laboratory. The infrared images in the experiments were all taken by FLIR infrared thermal imager, and the image sizes were all 1024×768. The experiments were conducted under MATLAB R2019a simulation software, with Windows 10 as the operating system, Intel Core i5-7300HQ as the CPU of the computer.

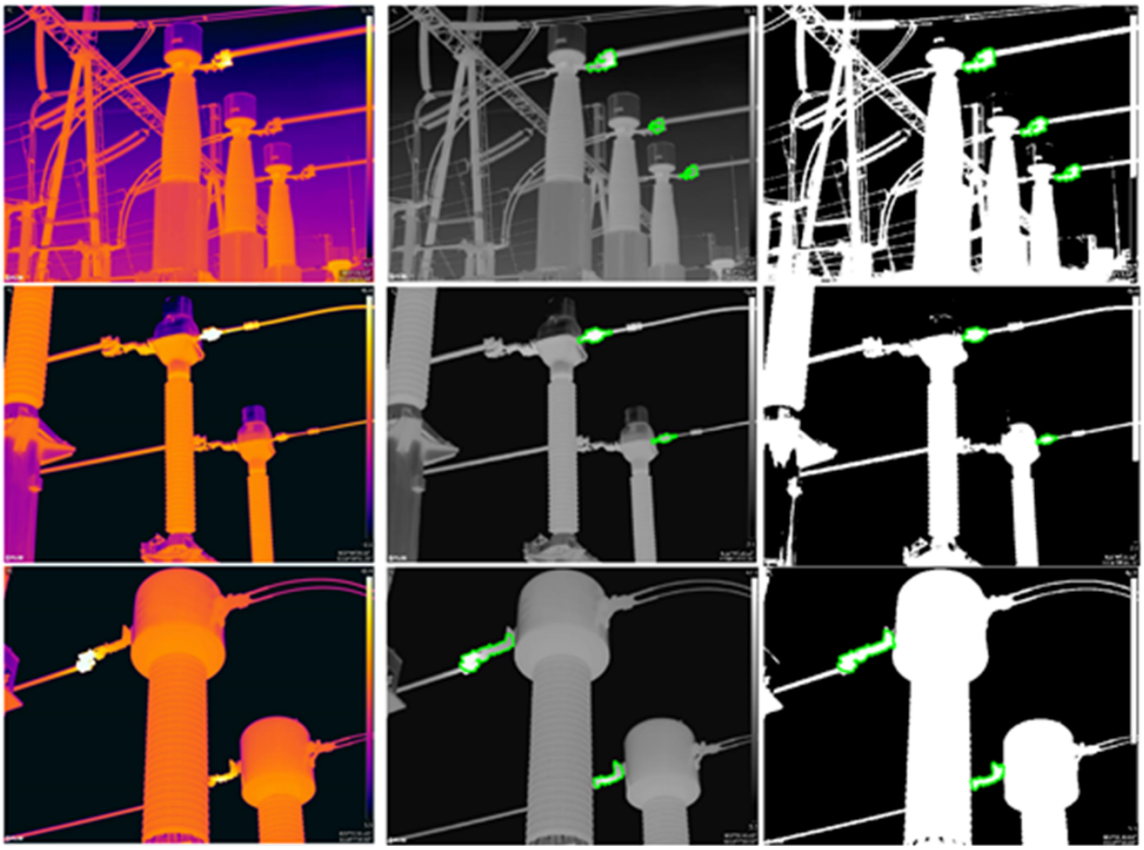

(a) Infrared image (b) CV model (c) Improved CV model

Fig.4 Experimental results

(1) Comparison of segmentation performance

CV model and the improved CV model were used to segment the hotline tap clamp of substation equipment in a substation. The main parameters of the segmentation model are set as follows: $\mu = 0.01/255^2$, $\nabla t = 1$, $\varepsilon = 1$. The infrared images are each set with the same initial profile of the level set. The results of the experimental part are shown in **Fig.4**, where the segmentation results are indicated by green lines. **Fig.4(a)** shows the original infrared image, **Fig.4(b)** shows the segmentation results of CV model, and **Fig.4(c)** shows the segmentation results of the improved CV model.

To compare the segmentation performance of CV model and the improved CV model, the segmentation efficiency and segmentation accuracy are compared and analyzed for 100 infrared images. Table 1 shows the comparison of the segmentation performance of the two models. We evaluate the model in terms of segmentation time consumption and segmentation accuracy.

Table.1 Comparison of the segmentation performance of two models

Infrared images	CV model	Improved CV model
Average time taken	89.67	**26.33**
Average JS Index	0.8177	**0.8638**

JS (Jaccard similarity) index is used to compare the segmentation accuracy of images. For all IR images, the average JS index is selected for analysis, and the results are shown in Table 1.

The segmentation evolution of hotline tap clamp using only CV model is inefficient. The improved CV model in this paper performs coarse segmentation of the image first by the two-dimensional Otsu algorithm, which reduces the scene complexity of CV model, improves the segmentation speed, and weakens the sensitivity of CV model to the initial conditions. Therefore, the segmentation takes less time and is more efficient.

From the comparison of the Average JS index in Table 1, we can see that the segmentation effect of the improved CV model is better than that of CV model. Because the Prewitt operator combines the differential information, the improved CV model has a better segmentation effect and noise immunity performance in image segmentation.

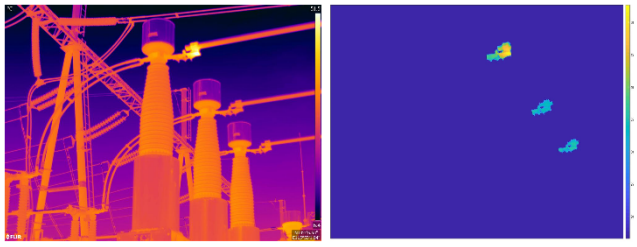

(a)Infrared image (b) Segmentation result

Fig.5 Experimental results

(2) Feasibility of fault warning algorithms

The main parameters of the splitting model are set as in experiment (1), and **Fig. 5** shows the experimental results. In the following analysis for **Fig. 5** by the relative temperature difference judgment method, the hotline tap clamp of the current transformer A-phase's temperature field anomalies and hot spots are obvious. The current ambient temperature T_0 is 20.00. The temperatures of current transformer A, B, C three-phase joints are 52.70, 26.64, and 26.37, respectively. And the normal phase corresponding point temperature T_2 is 24.32. According to equation (19), δ_1 can be calculated as 86.8%, 34.9%, 32.2%, and it can be seen that there is serious defect in the current transformer A phase in the image. It is recommended that substation arranges staff should overhaul in time, and inspect the current transformer B and C phases to prevent equipment failure. These experimental results verify the feasibility of the algorithm in this paper for early warning of faults in hotline tap clamp of substation equipment.

5. CONCLUSION

In this paper, in order to realize fault warning of hotline tap clamp of substation equipment, a hybrid segmentation method is proposed to realize the segmentation of hotline tap clamp in complex backgrounds. The method firstly preprocesses the infrared images through median filtering and grayscale routine. Then, we combine the real-time as well as global nature of 2D Otsu algorithm with the local optimality of CV model to reduce the scene complexity and improve the segmentation speed. CV model is not accurate enough for segmentation of images with uneven grayscale. Thus, the differential information obtained from the detection of target edges by the Prewitt operator is combined with CV model to improve the segmentation accuracy and solve the problems of blurred edge information of IR images and low efficiency of CV model operations. By using relative temperature difference judgment method and infrared detection judgment method, the early warning of hotline tap clamp of substation equipment is realized. According to the experiment results, the algorithm in this paper can maintain good edge continuity for the segmentation of hotline tap clamp of substation equipment in infrared images. The segmentation results have high accuracy, which can achieve the purpose of fault early warning according to the judgment criterion. This paper provides the basis and convenience for the subsequent structural area segmentation of substation equipment and the comparison of various data indicators of the corresponding parts.

ACKNOWLEDGEMENT

This work is supported by the Science and Technology Project of State Grid Corporation of China under Grant 5700-202118193A-0-0-00.

REFERENCES:

[1] C. Haomeng, "Application and Analysis of Infrared Temperature Measurement Technology in Judging Thermal Fault of Electrical Equipment," Electronic Test, no. 19, pp. 95-97, 2019.

[2] W. Miao, D. Wei, S. Hongbo and Z. Jing, "Transmission Line Fault Diagnosis Method Based on Infrared Image Recognition," Infrared Technology, vol. 39, no. 04, pp. 383-386, 2017.

[3] L. Wenpu, X. Ke, L. Xiao, L. Xiaoning and W. Hao, "Intelligent Diagnosis Method of Infrared Image for Transformer Equipment Based on Improved Faster R CNN," Southern Power System Technology, vol. 13, no. 12, pp. 79-84, 2019.

[4] X. Xiaohua, Q. Ping, W. Yida, Z. Xinyue, X. Hanlin and X. Libing, "Multi — granularity hazard detection method for electrical power system," Journal of Beijing University of Aeronautics and Astronautics, vol. 47, no. 03, pp. 520-530, 2021.

[5] Y. Zhaoguang, Z. Zhongyuan, W. Dingjun, Z. Xi, L. Xiang and W. Ye, " R esearch on Image Segmentation and Fault Diagnosis of Infrared Detection in Substation Equipment," BULLETIN OF SCIENCE AND TECHNOLOGY, vol. 35, no. 03, pp. 95-99, 2019.

[6] W. Xiaofang and M. Huamin, "Infrared Image Segmentation Method for Power Equipment in Complex Background," Infrared Technology, vol. 41, no. 12, pp. 1111-1116, 2019.

[7] Y. Chou and L. Yao, Automatic Diagnosis System of Electrical Equipment using Infrared Thermography, IEEE Computer Society, 2009, pp. 155-160.

[8] G. Pengcheng and H. Fuzhen, "Power equipment infrared image segmentation based on improved Chan- Vese model," Computer Engineering and Applications, vol. 53, no. 10, pp. 193-196, 2017.

[9] W. Xiaofang, K. Chen, C. Hongbo, Z. Han, X. Jianbo and J. Qingzhao, "Automatic Diagnosis Method for Thermal Faults of Substation Equipment Based on Infrared Image Processing," Journal of East China Jiaotong University, vol. 36, no. 03, pp. 111-118, 2019.

[10] C. Jishun, X. Lijun, W. Xinyu, M. Ruijie, Q. Huiping and L. Lei, "Research on Enhancement and Segmentation of Power Equipment Infrared Heat Map in Complex Environment," Infrared Technology, vol. 40, no. 11, pp. 1112-1118, 2018.

[11] T. Tsai, S. Su and T. Lee, "Fast Mode Decision Method Based on Edge Feature for HEVC Inter-Prediction," IET Image Processing, vol. 12, no. 5, pp. 644-651, 2018, doi: https://doi.org/10.1049/iet-ipr.2016.1117.

[12] H. Shizheng, "Method and Criterion of Relative Temperature Difference Determination of Infrared Diagnosis for Electric Equipment," Power System Technology, no. 10, pp. 49-52, 1998.

[13] O. Nobuyuki, "A Threshold Selection Method from Gray-Level Histograms," IEEE Transactions on Systems, Man, and Cybernetics, vol. 9, no. 1, pp. 62-66, 1979, doi: 10.1109/TSMC.1979.4310076.

[14] L. Yajun and C. Xuejun, "Fault zone extraction of electrical equipment by using PCNN based on Otsu optimization," Journal of Fujian University of Technology, vol. 18, no. 06, pp. 593-597, 2020.

[15] F. Jiulun and Z. Feng, "Two-Dimensional Otsu's Curve Thresholding Segmentation Method for Gray-Level Images," Acta Electronica Sinica, no. 04, pp. 751-755, 2007.

[16] G. Haitao, W. Lianyu, T. Tan, Z. Chuntian and S. Hequan, "Automatic Thresholding Using the Otsu Algorithm Based on the Two-Dimensional Bound Histogram," Journal of Optoelectronics·Laser, no. 06, pp. 739-742, 2005.

[17] T.F. Chan, B.Y. Sandberg and L.A. Vese, Active Contours without Edges for Vector-Valued Images, Academic Press, 2000, pp. 130-141.

[18] V.V. Terzija and H.-J. Koglin, "On the Modeling of Long Arc in Still Air and Arc Resistance Calculation," IEEE Transactions on Power Delivery, vol. 19, no. 3, pp. 1012-1017, 2004, doi: 10.1109/TPWRD.2004.829912.

[19] Z. Yang, T. Kelun, L. Yan, B. Xiaoli and L. Jipeng, "An Improved Active Contour Model Based on C-V Model," Journal of Sichuan University of Science & Engineering(Natural Science Edition), vol. 27, no. 05, pp. 33-36, 2014.

[20] P. Zhen, W. Zhenzhou, X. Da, S. Yongcan, W. Zihao and L. Yikang, "A Method of UV Image Segmentation for Corona Discharge Based on C-V Model," Science Technology and Engineering, vol. 20, no. 14, pp. 5661-5666, 2020.

[21] Z. Xiaoli, Z. Pucheng and X. Mogen, "A Kind of Infrared Image Segment Method Using Improved Chan-Vese Model," Infrared Technology, vol. 38, no. 09, pp. 774-778, 2016.